Proc. Natl. Acad. Sci. USA
Vol. 84, pp. 2737–2741, May 1987
Biophysics

Role of "active" potassium transport in the regulation of cytoplasmic pH by nonanimal cells

(intracellular pH/K^+–H^+ cotransport/electrogenic H^+ pump/current–voltage analysis/*Neurospora*)

MICHAEL R. BLATT* AND CLIFFORD L. SLAYMAN

Department of Physiology, Yale University School of Medicine, 333 Cedar Street, New Haven, CT 06510

Communicated by Winslow R. Briggs, December 29, 1986 (received for review June 9, 1986)

ABSTRACT **High-affinity potassium uptake in *Neurospora* occurs by symport with protons [K_m (apparent) = 15 μM at pH 5.8], for which a large inward gradient (≈400 mV) is generated by the H^+-extruding ATPase of the plasma membrane. Operating in parallel, the two transport systems yield a net 1:1 exchange of K^+ for cytoplasmic H^+. Since this exchange could play a role in cytoplasmic pH (pH_i) regulation, the coordinated functioning of the K^+–H^+ symport and H^+ pump has been examined during acid stress. Cytoplasmic acid loads were imposed by injection and by exposure to extracellular permeant weak acid. Multibarrelled microelectrodes were used to monitor membrane potential (V_m), pH_i, and the current–voltage (*I–V*) characteristics of the cells. The behaviors of the H^+ pump and K^+–H^+ symport were resolved, respectively, by fitting whole membrane *I–V* curves to an explicit kinetic model of the *Neurospora* membrane and by subtracting *I–V* curves obtained in the absence from those obtained in the presence of 5–200 μM K^+ outside. Proton pumping accelerates nearly in proportion with the cytoplasmic H^+ concentration, but pH_i recovery from imposed acid loads is dependent on micromolar K^+ outside. Potassium import via the symport leads to a measurable alkalinization of the cytoplasm in accordance with stoichiometric (1:1) K^+/H^+ exchange. Potassium transport is accelerated at low pH_i, but in a manner consistent with its inherent voltage sensitivity and changes in V_m resulting from an increased rate of H^+ extrusion by the pump. The primary response to acid stress thus rests with the H^+ pump, but K^+ transport introduces an essential kinetic "valve" that can regulate net H^+ export.**

A feature common to all living cells is the ability to maintain cytoplasmic pH (pH_i) nearly constant in the face of a continuous acid load. Normal metabolic processes ensure that most cells are net acid producers (1). In the short term and for small acid loads, chemical buffering of proteins and other cytoplasmic components will stabilize pH_i; but in the long term, metabolic acid production implies cellular mechanisms for net export of H^+.

In animal cells, for which membrane transport is coupled primarily to Na^+ gradients generated by the Na^+/K^+-ATPase, acid export generally is accomplished by transport-mediated exchange of Na^+ for H^+ and Cl^- for HCO_3^- (2). By contrast, the transport economies of eukaryotic cells with walls and of prokaryotes are generally based on the electrochemical potential difference for protons ($\bar{\mu}_{H^+}$), a fact that has fueled arguments (3) that primary H^+ pumps could regulate pH_i. Conceivable, too, are circumstances in which "the demonstrated task of maintaining a large $\bar{\mu}_{H^+}$ and the postulated task of regulating pH_i could not be accomplished by the same ion pump" (4). In fact, it is now known that bacteria control pH_i via membrane transporters that are distinct from the proton pumps (5, 6).

For plants and fungi, the notion that H^+ pumping alone can account for pH_i control remains at issue (7–9). In the best documented example, *Neurospora*, acid loading stimulates the H^+ pump, but pump activity does not appear essential for stabilizing pH_i (8). The situation is complicated further by widespread observations of net H^+ export associated with K^+/H^+ exchange and its stimulation under acid stress in higher plants (10), algae (11), and yeast (12). Cytoplasmic alkalinization is frequently (13, 14) though not always (15) observed during K^+ uptake, at least with 10–100 mM extracellular K^+ (K_o^+). K^+/H^+ exchange is most evident, however, in cells partially depleted of K^+. These cells exhibit low values for pH_i (16) and apparent Michaelis constants of 10–30 μM for K^+ import (10, 17). Initially it was held that acid loads might stimulate an electroneutral K^+/H^+ exchange system necessarily fueled by ATP hydrolysis to drive both H^+ and K^+ against their respective thermodynamic gradients (18). The notion of an H^+/K^+-ATPase, however, has remained unconvincing (see ref. 19 for a review). So, in plants and fungi, the mechanism by which potassium is "actively" transported and its role in pH_i homeostasis have remained open questions.

Recently, a high-affinity transport system was identified in *Neurospora* that carries K^+ inward in cotransport with H^+ (19), analogous to one bacterial system (20). Transporter activity was observed after a period of K^+ starvation, and the porter was capable of supporting cytoplasmic K^+ levels of 60–100 mM with 2–10 μM K_o^+. Charge balance was maintained by the electrogenic H^+ pump, giving rise to a net exchange of K_o^+ for intracellular H^+ (H_i^+) as measured extracellularly. The possibility that such a K^+–H^+ symport could account for much of the K^+ transport behavior of higher plants, algae, and fungi raises the issue of its role in regulating pH_i. In this paper we examine the relationships between pH_i, K^+–H^+ cotransport, and the H^+ pump in *Neurospora*, with emphasis placed on the physiological consequences of cytoplasmic acid loading. Our results show that in K^+-depleted cells, primary H^+ pumping and parallel, secondarily coupled K^+ movements are competent to maintain pH_i near neutrality.

MATERIALS AND METHODS

Cells and Protocol. Spherical cells of the normally mycelial fungus *Neurospora*, wild-type RL21a, were grown in ammonium phosphate-containing Vogel's medium (initial K^+ concentration, 0.3 mM) with 1% glucose and 18% ethylene glycol for 3 days (19). On harvesting, the cells (diameters, 15–20

The publication costs of this article were defrayed in part by page charge payment. This article must therefore be hereby marked "*advertisement*" in accordance with 18 U.S.C. §1734 solely to indicate this fact.

Abbreviations: pH_i, intracellular pH; K_o^+, extracellular potassium; V_m, membrane potential; *I–V*, current–voltage (relationship); ΔI–V, difference current–voltage (relationship); H_i^+, intracellular H^+.

*Present address: Department of Botany, University of Cambridge, Downing Street, Cambridge CB2 3EA, United Kingdom.

μm) were washed free of ethylene glycol and resuspended in K^+-free buffer containing 10 mM Mes [2-*N*-(morpholino)ethanesulfonic acid] titrated to pH 5.8 with $Ca(OH)_2$ (Ca^{2+}-Mes; K^+ concentration, 0.5–0.8 μM). Electrical measurements were carried out in continuously flowing solution, and K_2SO_4 was added by rapid secondary flow (19). Acetate, when present, was added as the free acid titrated to pH 5.8 with $Ca(OH)_2$.

Electrodes, pH Measurement, and H^+ Injection. Multibarrelled microelectrodes were manufactured and used as previously described (22). For pH_i measurements, three-barrelled electrodes were made to include one barrel containing tri-(*n*-dodecyl)amine, a pH-sensitive, ion-exchanger (Fluka, Buchs, Switzerland). Polyvinyl chloride (10% wt/vol) stabilized the exchanger against cell-turgor pressure. Calibrations were carried out in 20 mM sodium phosphate buffers with (and without) 50 mM KCl. Electrodes were selected that gave >54 mV per pH unit (pH 5–8) and 90% response times < 15 s. The remaining two barrels were filled with 50 mM KOAc (pH 7.1) and were used for voltage-clamping and recording. For H^+ injections four-barrelled electrodes were used, of which one barrel was filled with 10 mM H_2SO_4 and one with 20 mM KOAc. These barrels were connected by Ag-AgCl|KCl half cells to a custom-made iontophoresis unit.

Current–Voltage (*I–V*) Measurements and Kinetic Analysis. The *I–V* characteristic of the plasma membrane was determined by computer-controlled voltage clamp using the two-electrode method. *I–V* curves obtained with and without K_o^+ were used to obtain the difference [Δ*I–V*] curves for K^+–H^+ cotransport by current subtraction over the entire voltage span (26). Ionic (chemical) fluxes occurring in non-voltage-clamped cells could be referenced directly to the current difference at V_m in K_o^+. In addition, *I–V* curves recorded in the absence of K_o^+ were decomposed into "pump" and "leak" components, assumed to function electrically in parallel (4, 24). The nonlinear leak was described empirically by a composite Goldman relation defined by a "permeability" (P_L) and an equilibrium potential (E_L). The H^+ pump was represented as a three-state carrier cycle in which all reaction steps not directly associated with membrane charge transit or H_i^+ binding were lumped together. Hence, the pump (carrier density *N*) comprised three pairs (forward and backward) of reaction constants, two each describing membrane charge transit (k_{12}, k_{21}), H_i^+ loading/unloading (k_{31},k_{13}), and the lumped voltage-independent steps (κ_{23}, κ_{32}). Voltage dependence was assigned to a symmetric Eyring barrier (21) so that $k_{12} = k_{12}^0\exp(zFV_m/2RT)$ and $k_{21} = k_{21}^0\exp(-zFV_m/2RT)$, where k_{12}^0 and k_{21}^0 are the rate constants at zero membrane potential ($V_m = 0$) and z (=1), F, R, and T have their usual meanings. Full equations for the total membrane (i_m), leak (i_L), and pump (i_P) currents were

$$i_m = i_P + i_L, \qquad [1]$$

where

$$i_L = \frac{F^2}{RT}P_L C_i V_m \frac{1 - \exp(-F(V_m - E_L)/RT)}{1 - \exp(-FV_m/RT)}, \qquad [2]$$

and C_i is the intracellular concentration of a putative leakage cation.

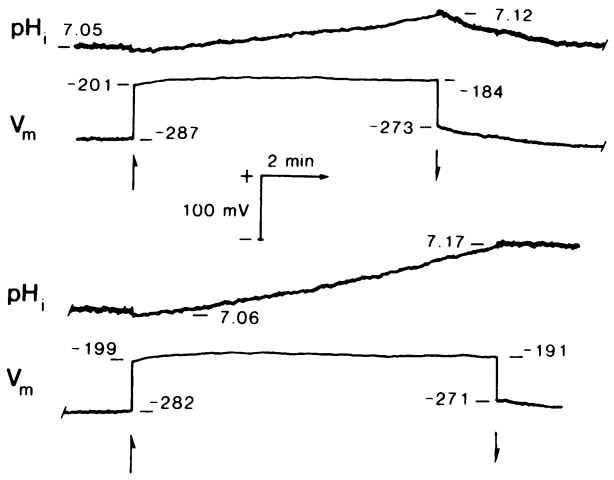

FIG. 1. Membrane potential and pH_i traces from one cell in 10 mM Ca^{2+}-Mes, pH 5.8. The voltage scale applies to the V_m traces only. Cytoplasmic alkalinization was evident only in the presence of K_o^+ (50 μM; ↑, addition; ↓, subtraction) in this and all other experiments. Initial 0.06 pH-unit acid drift followed the first removal of K_o^+ (the time in K^+-free medium between K_o^+ exposures shown was 12.6 min). The slight downward displacement of the pH_i trace in K_o^+ reflects a 0.1% gain mismatch between amplifiers.

All parameters (k_{12}^0, k_{21}^0, k_{13}, k_{31}, κ_{23}, κ_{32}, P_L, and E_L) were found by least-squares fitting of Eq. **1** jointly to sets of *I–V* curves obtained at intervals during acid loading and washout.

RESULTS

pH_i in K^+-Starved Cells and Its Response to K^+ Transport. The cytoplasmic pH recorded on impalement of K^+-starved spherical cells [7.02 ± 0.06 (n = 10)] was about 0.2 pH unit lower than reported for K^+-replete *Neurospora* (8). Responses of pH_i and V_m to 50 μM K_o^+ are shown in Fig. 1. K_o^+ elicited large and rapid positive shifts in V_m associated with current through the K^+–H^+ symport (19). After prolonged exposure to K_o^+, V_m recovered only partially on initial transition to K^+-free buffer (see also Fig. 2). In Ca^{2+}-Mes buffer alone, pH_i remained constant or, immediately after K_o^+ washout, decreased slowly. Addition of 50 μM K_o^+ resulted in a steady 0.019 ± 0.008 pH unit per min increase in pH_i (n = 8; the longest single period in K_o^+ was 17.8 min).

Charge Stoichiometry of K_o^+/H_i^+ Exchange. In establishing a charge stoichiometry for K^+ transport of two positive charges per K^+ [2(+):1(K^+)], Rodriguez-Navarro *et al.* (19) found K^+ efflux was <20% of the cation influx for 5–200 μM K_o^+. So it was expected that the same charge stoichiometry would hold for K^+/H^+ exchange: 2(+) charges [and 1(K^+)] should enter the cell for each H^+ exported (net). Buffering of pH_i precluded directly comparing K^+ transport currents (obtained by current subtraction) with net H^+ movements. Instead, simultaneous *I–V* and pH_i recordings were used to calculate the pH-buffering capacity, β, of the cytoplasm *assuming* a charge stoichiometry of 2(+):1(H^+); the result

$$i_P = zFN \frac{k_{12}\kappa_{23}k_{31} - k_{21}\kappa_{32}k_{13}}{k_{12}(\kappa_{23} + \kappa_{32} + k_{31}) + k_{21}(k_{13} + k_{31} + \kappa_{32}) + k_{13}(\kappa_{23} + \kappa_{32}) + k_{31}\kappa_{23}}, \qquad [3]$$

then could be compared with independent and more conventional estimates of β by using the Henderson–Hasselbalch

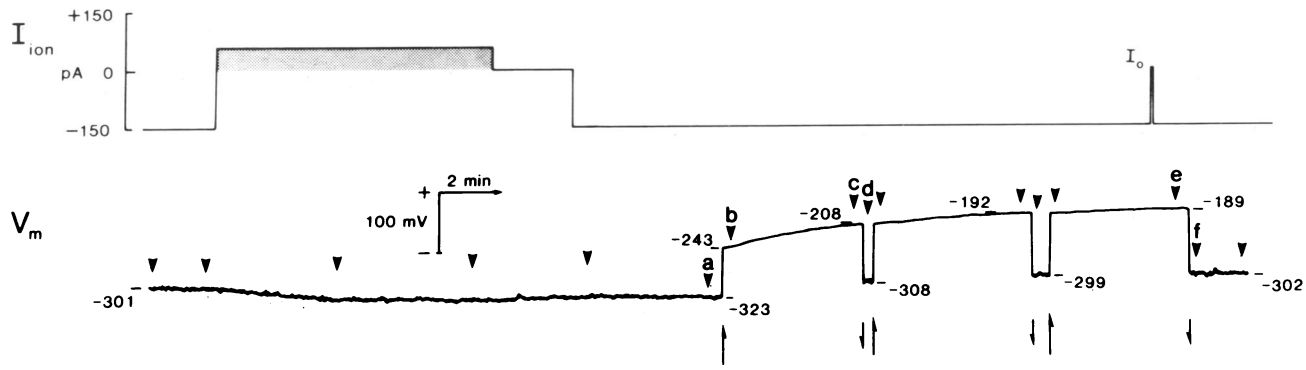

FIG. 2. Membrane potential V_m and iontophoresis current I_{ion} traces during acid loading and washout. Positive current (shaded, 45-pA injection) released HOAc and negative current (150-pA backing) released K_2SO_4 into the cell. ↑ and ↓ below V_m trace, addition and subtraction, respectively, of 50 μM K_o^+; arrowheads above V_m trace mark *I–V* scans (duration, 6.4 s). *I–V* scans a–f refer to Figs. 3–5. At I_0, the backing current was switched off as a check against voltage offset in V_m. The acid load was 0.13 pmol of H^+ (assumed transport number, 0.5; diffusional contributions were ignored) and K^+ import was 0.14 pmol (mean symport current, 2.1 μA cm^{-2}; cell surface area, 1464 μm^2); these values were estimated by integrating I_{ion} and the symport current over time. From the cell volume (5.3 pl), a cytoplasmic buffering capacity of 34–36 mM H^+ per pH unit was obtained.

equation and pH_i recorded from the same cell exposed to permeant weak acid (2, 8).

For measurements based on external weak acid loading, 5 mM acetate (pK_a = 4.77) was used because propionate and butyrate (4, 8) introduced large, voltage-gated conductances in spherical cells. Control experiments showed that acetate did not stimulate respiration in the cells beyond that expected from its effect on pH_i and hence on H^+-ATPase turnover rate (25). Also, continuous injections of KOAc (pH 7.1) over 10–30 min had no measurable effect on the membrane *I–V* characteristic.

Experiments with two cells were carried out combining both approaches to estimate β. The first cell yielded values of 157 (symport current) and 152 mM H^+ (weak acid) per pH unit; in the second cell, exposure to acetate was bracketed by current measurements that gave 40 and 45 mM H^+ per pH unit. Acetate loading gave 41 mM H^+ per pH unit. The 3.5-fold difference in β between cells was surprising at first, but records from an additional five cells indicated a wide spread in buffer capacities (137 ± 25; range of 61–202 mM H^+ per pH unit). Within this range, the values accorded with known effects of carbon starvation in *Neurospora* (D. Sanders, personal communication). By contrast, disparities between measurements from the individual cells (worst case, 10% of the acetate-derived values) were well within the 20% margin set by K^+ efflux. The results thus supported the 2(+):1(H^+) relationship on which the calculations were based and the underlying assumption of K^+ import in cotransport with H^+.

Response of K^+ Transport to pH_i. One outstanding feature of K^+–H^+ cotransport is its voltage-dependence. In micromolar K_o^+ the transport velocity (current) increases roughly 10-fold as the membrane hyperpolarizes (voltage increases negatively) from −100 to −300 mV, precisely over the normal physiological voltage range. Consequently, there are two ways in which pH_i might affect K^+ transport: (*i*) pH_i might regulate transport *directly* by altering the symport kinetics, or (*ii*) it might influence transport rates *indirectly*—within existing kinetic bounds—through acid-induced changes in V_m.

To address both possibilities at once, we acid-loaded single spherical cells by iontophoretic injection of H^+ (co-injected anion OAc^-) in the absence of K_o^+ and then let the cells recover in micromolar K_o^+. Whole membrane *I–V* curves, obtained at intervals throughout each experiment, were used to extract the voltage-dependent kinetic features of the H^+-pump and K^+–H^+ symport. Technical considerations prohibited combining pH_i recording and iontophoretic injections; but analogous experiments with pH microelectrodes, carried out by acid loading with 5 mM OAc^- in the bathing medium, indicated H^+-pump stimulation to be quantitatively consistent with simple H^+-substrate enhancement (see ref. 4 and Fig. 5). So, the pump *I–V* characteristic could be used to index changes in pH_i on injection. The experiments with acetate also gave results with respect to K^+ transport that were similar to those obtained by acid injections (see below) when measurements in the presence and absence of the weak acid were compared.

Figs. 2–5 show the results of an acid load/washout cycle from one cell (H^+-injected twice previously over 1.2 hr). For clarity, analyses for acid washout only are illustrated. (Preinjection control *I–V* curves and fittings were superimposable with the *I–V* data of curves e/f and are included in Fig. 3 *Inset* along with data from the preceding load/washout cycle.) Acid injection (Fig. 2) shifted V_m from −301 to −323 mV. Both potential and associated membrane *I–V* profiles (see below) were retained in the absence of K_o^+ (7.8 min; and in the preceding load/washout cycle, 11.3 min), even with a 150-pA backing current applied subsequently to prevent diffusional H^+ leakage from the electrode.† Addition of 50 μM K_o^+ restored V_m and the *I–V* profile (recorded in K^+-free buffer) to their preinjection levels in about 13.7 min.

Potassium transport was stimulated *per se* by H^+ injection in the otherwise non-voltage-clamped cell. Symport current at V_m prevailing in the presence of K_o^+ increased 2.3-fold, declining subsequently as pH_i recovered (Fig. 3). Even so, essentially all of the effect of acid loading on the symport could be attributed to changes in V_m. No appreciable differences in the voltage-dependent kinetic (Δ*I–V*) characteristic for K^+ transport were seen during acid loading or washout (Fig. 4).

By contrast, fitting whole membrane *I–V* curves taken in K_o^+-free buffer to Eq. 1 showed a marked displacement of the pump *I–V* characteristic, which recovered during K^+ exposure (Fig. 5). Especially satisfying was the fact that the best fittings in this and three other experiments (also two cells acid-loaded with acetate) were obtained by varying one

†Estimates of H^+ diffusion based on electrode geometry and resistance (27, 28) suggested a leakage rate of 0.1–0.2 fmol·s^{-1}, for which the backing current [1.6 feq·s^{-1} (eq = equivalents)] would have compensated amply. However, pump *I–V* curves in this and one other experiment indicated a slow decrease in pH_i initially after K_o^+ removal (see also Fig. 1). Since K_o^+ accelerates H^+ extrusion and hence ATP consumption by the H^+ pump, one likely source of acid is metabolic CO_2. Nonetheless, recovery from H^+ injection was greatly accelerated by micromolar K_o^+.

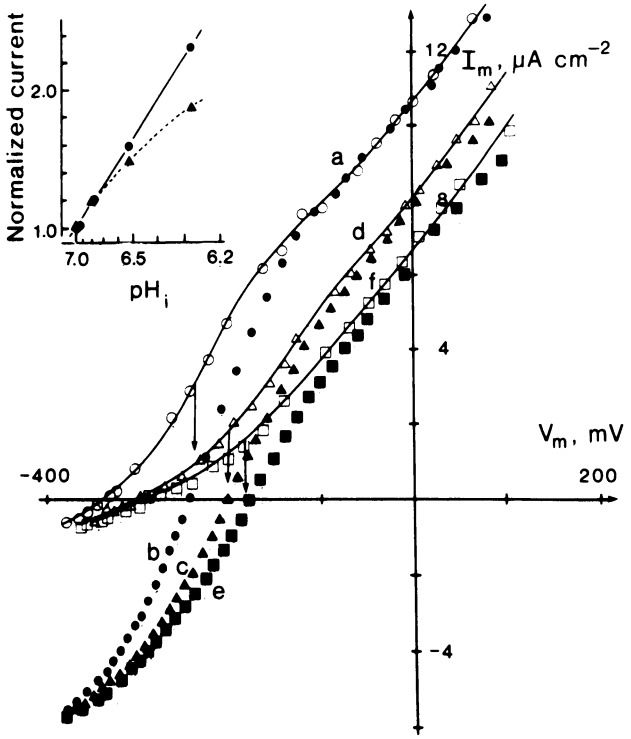

FIG. 3. Whole membrane *I–V* curves recorded during acid washout (Fig. 2) without (curves a, d, and f) and with (curves b, c, and e) 50 μM K_o^+. Curves a, d, and f were fitted to Eq. 1 (see Fig. 5). ↓, Prevailing symport currents at V_m. (*Inset*) Pump (▲) and symport (●) currents at V_m, normalized and plotted against the acid load. Pump current and relative pH_i [$= -\log(k_{31}/k_{31,initial})$] were from the corresponding data in Fig. 5; a control of $pH_i = 7.0$ was assumed. Preinjection currents were 1.61 (pump) and 1.25 (symport) μA·cm^{-2}. Points from the preceding load/washout cycle are included in the analysis.

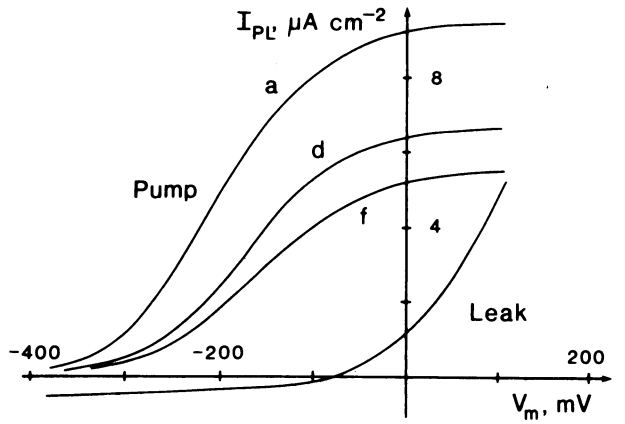

FIG. 5. H^+ pump response during acid washout and to known acid loads. Fitted pump curves a, d, and f refer to those in Fig. 3. Data with recorded pH_i were taken from one of two separate cells exposed to 5 mM acetate. Unaffected parameters of the acetate loaded cell are shown in parentheses: P_L, 4.69×10^{-7} (5.67×10^{-7}) cm·s^{-1}; E_L, −84 (−87) mV; k_{12}^0, 2.48×10^4 (8.06×10^4) s^{-1}; k_{21}^0, 1.24×10^{-3} (1.88×10^{-3}) s^{-1}; κ_{23}, 10.6 (12.6) s^{-1}; κ_{32}, 0.11 (4.03) s^{-1}; k_{13}, 2.64×10^3 (211) s^{-1}. Affected parameter and related functions are as follows:

Curve or pH_i	Membrane potential, mV	Equilibrium potential, mV	Saturating current, μA·cm^{-2}	k_{31} ($=k_{31}^0[H^+]_i$), s^{-1}
a	−323	−443	9.17	67.7
d	−308	−413	6.96	20.5
f	−302	−402	5.76	12.8
6.61	−301	−424	10.82	24.4
6.98	−297	−406	9.43	12.0
7.06	−286	−401	8.93	9.81
7.10	−283	−396	8.57	8.58

Slope (k_{31} vs. pH_i) was 10.89 per $[H^+]_i$ decade (regression coefficient, 0.993).

reaction constant only, k_{31}, which represents H^+ binding at the cytoplasmic surface of the membrane. For the experiment illustrated, the fitting indicated a −41 mV shift in the pump equilibrium potential (24), a 5.3-fold rise in the reaction constant k_{31}, and, hence, a −0.72-unit (acid) shift in pH_i ($[H^+]_i/[H^+]_{i,initial} = k_{31}/k_{31,initial}$) on injection. Furthermore, the fitted pump current balanced the sum of the leak and K^+–H^+ symport currents at V_m prevailing in the presence of K_o^+ (the error was <3% of the sum; see Figs. 3–5). So, changes in V_m both during acid loading and during washout in the presence of K_o^+ were accounted for quantitatively by pH_i-dependent modulation of pump kinetics.

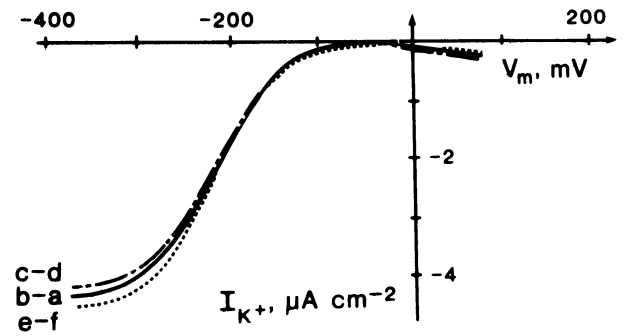

FIG. 4. K^+–H^+ symport response during acid washout. Δ*I–V* curves were obtained by subtraction (b−a, c−d, e−f) using 4th-order spline interpolation of the data sets in Fig. 3. Failure of the curves to cross the voltage axis at the symport equilibrium potential (about −85 to −50 mV) is a consequence of subtraction and does not affect interpretation of the curves at more negative potentials (26).

DISCUSSION

Controlling Net H^+ Export Under Acid Stress. The results presented above identify a simple transport loop, comprising electrogenic H^+ pumping in parallel with secondary π_{H^+}-coupled transport, and its role in pH_i recovery from acid stress in nonanimal eukaryotic cells. The primary response to acid loading rests firmly with the H^+ pump. The observed increase in pump activity is kinetically consistent with the increase in free solute (H_i^+) concentration for translocation and constitutes an overall rise in the rate of H^+ movement through the pump at the prevailing V_m. Nonetheless, the efficacy of this response is severely restricted without external K^+; it is current circulation through the K^+–H^+ symport that results in a *net* H^+ export and that provides a primary level of control on its rate in these experiments. A central feature of the transport loop, therefore, lies in stress-related operational coupling of pump and symport. To understand each component and its role in pH_i recovery, it is necessary to examine the kinetic features of the two transport systems, both in relation to each other and in relation to the *Neurospora* membrane as a whole.

Membrane potential, in addition to the chemical substrates K^+ and H^+, plays a key role in the kinetic behavior of the H^+ pump and K^+–H^+ symport. Pump velocity (current) is voltage-dependent and declines over the physiological voltage range at potentials negative of −100 mV. One important consequence of this fact is that increasing pump activity against a constant leak conductance drives V_m to more negative values (until pump and leak currents are once again equal) and thereby limits the extent to which pump velocity may rise with $[H^+]_i$. This behavior underlines the inadequacy

of stimulating the H^+ pump alone: the pump is unable to keep pace with large proton loads (see Fig. 3 *Inset*). Then, too, the leak itself may reflect a finite conductance to H^+ (29). So, accelerating the pump might do little more than increase the rate of H^+ return via the leak.

By contrast, linking current circulation through the pump with K^+–H^+ cotransport clearly is a successful means to cope with acid stress for at least three reasons. First and foremost, the K^+–H^+ symport defines an "open circuit" in *proton* circulation through the membrane; parallel operation of symport and pump yields net H^+ *export* (K^+/H^+ exchange), even though K^+ uptake is coupled mechanistically to H^+ *reentry*. Second, the symport is strongly depolarizing. In the presence of micromolar K_o^+, V_m is shifted far positive and, consequently, the H^+ pump is less compromised by its own voltage sensitivity.

The relationship between pump and symport is still more subtle, however, and the third point relates to the voltage-dependence of K^+–H^+ cotransport itself. Membrane potential exerts its most pronounced effects on pump and symport over the same voltage range, but the two currents are inversely related: increasing V_m (negative) *increases* symport current. Furthermore, symport current is a nonlinear function of voltage; symport conductance increases with negative voltage (the maximum in 50 μM K_o^+ is near -250 mV). Together, these features compensate for the voltage-limited response of the pump (Fig. 3 *Inset*) and introduce a voltage-dependent, kinetic "valve" on net H^+ export. As the cytoplasmic acid load rises and V_m increases (inside negative) with H^+-pump activity, both total current circulation through the membrane and the *proportion* of that current associated with net H^+ export increase (compare leak and symport profiles, Figs. 4 and 5), even without a direct effect of pH_i on K^+–H^+ symport kinetics.

Implications for K^+ Transport and Homeostasis. H^+ pump/K^+–H^+ symport coordination provides a coherent framework unifying many observations of pH_i-dependent K^+ transport and of K^+-stimulated H^+ pumping in plants, algae, and fungi. It also raises fundamental questions relating to transport control, pH_i and K_i^+ homeostasis. Significantly, the *Neurospora* K^+–H^+ symport is relatively insensitive to internal ligand (H^+ and K^+) concentrations (Fig. 4; also ref. 19). Kinetic sensitivity to pH_i would compromise any role of the symport in pH_i homeostasis.

It is important now to examine whether, in K^+-replete cells, the symport is activated under acid stress. The previous study (4) of *Neurospora* during acid-loading implicated a pH_i-mediated and time-dependent change in the leak conductance. At the time, demonstrating transport-dependent recovery from acid stress was not possible, and high-affinity K^+ transport was not suspected. Leakage of organic acid anions out of the cell to balance charge movement through the pump was the favored explanation, but in retrospect activation of K^+–H^+ cotransport is conceivable. Similarities in the conductance–voltage profiles for pump and symport mean that the latter might have been mistakenly attributed to the pump in curve fitting.

An equally important issue relates to K^+ circulation through the membrane. If K^+/H^+ exchange is a common means for pH_i control, K^+ import implies a separate mechanism for K^+ export in K^+-replete cells. There is limited evidence for ion-coupled K^+ transport in yeast, which could fill this role (12, 23). However, in the present context, K^+ export is unlikely to occur either by simple diffusion (uniport) or by exchange for H^+. Either mechanism would lead to futile circulation of both cations through the membrane and would defeat any function in pH_i homeostasis.

We thank Drs. A. Rodriguez-Navarro (Cordoba) and D. Sanders (York) for many helpful discussions and Dr. E. A. C. MacRobbie (Cambridge) for her support during the preparation of the manuscript. This work was supported by National Institute of General Medical Sciences Grant GM15858, by Department of Energy Grant DEFG02-85ER3359, and by National Research Service Award AM07259 to M.R.B.

1. Lehninger, A. L. (1970) *Biochemistry* (Worth, New York).
2. Roos, A. & Boron, W. F. (1981) *Physiol. Rev.* **61,** 296–434.
3. Smith, F. A. & Raven, J. A. (1979) *Annu. Rev. Plant Physiol.* **30,** 289–311.
4. Sanders, D., Hansen, U.-P. & Slayman, C. L. (1981) *Proc. Natl. Acad. Sci. USA* **78,** 5903–5907.
5. Padan, E., Zilberstein, D. & Schuldiner, S. (1981) *Biochim. Biophys. Acta* **650,** 151–166.
6. Zilberstein, D., Agmon, V., Schuldiner, S. & Padan, E. (1982) *J. Biol. Chem.* **257,** 3687–3691.
7. Roberts, J. K. M., Ray, P. M., Wade-Jardetsky, N. & Jardetsky, O. (1981) *Planta* **152,** 74–78.
8. Sanders, D. & Slayman, C. L. (1982) *J. Gen. Physiol.* **80,** 377–402.
9. Reid, R. J., Field, L. D. & Pitman, M. G. (1985) *Planta* **166,** 341–347.
10. Poole, R. J. (1978) *Annu. Rev. Plant Physiol.* **29,** 437–460.
11. Tromballa, H. W. (1978) *Planta* **138,** 243–248.
12. Pena, A. (1975) *Arch. Biochem. Biophys.* **167,** 397–409.
13. Conway, E. & Downey, M. (1950) *Biochem. J.* **47,** 355–360.
14. Ogino, T., den Hollander, J. A. & Shulman, R. G. (1983) *Proc. Natl. Acad. Sci. USA* **80,** 5185–5189.
15. Roberts, J. K. M., Wemmer, D., Ray, P. M. & Jardetsky, O. (1982) *Plant Physiol.* **69,** 1344–1347.
16. Pena, A., Cinco, G., Gomez-Puyou, A. & Tuena, M. (1972) *Arch. Biochem. Biophys.* **153,** 413–425.
17. Borst-Pauwels, G. W. F. H. (1981) *Biochim. Biophys. Acta* **650,** 88–127.
18. Leonard, R. T. (1982) *Membr. Transp.* **2,** 633–637.
19. Rodriguez-Navarro, A., Blatt, M. R. & Slayman, C. L. (1986) *J. Gen. Physiol.* **87,** 649–674.
20. Bakker, E. & Harold, F. M. (1980) *J. Biol. Chem.* **255,** 433–440.
21. Lauger, P. & Stark, G. (1970) *Biochim. Biophys. Acta* **211,** 458–466.
22. Blatt, M. R. & Slayman, C. L. (1983) *J. Membr. Biol.* **72,** 223–234.
23. Ortega, M. D. & Rodriguez-Navarro, A. (1985) *Z. Naturforsch.* **402,** 721–725.
24. Hansen, U.-P., Gradmann, D., Sanders, D. & Slayman, C. L. (1981) *J. Membr. Biol.* **63,** 165–190.
25. Gradmann, D., Hansen, U.-P., Long, W. S., Slayman, C. L. & Warnke, J. (1978) *J. Membr. Biol.* **39,** 333–367.
26. Blatt, M. R. (1986) *J. Membr. Biol.* **92,** 91–110.
27. Geisler, C. D., Lightfoot, E. N., Schmidt, F. P. & Sy, F. (1972) *IEEE Trans. Biomed. Eng.* **19,** 372–375.
28. Hodgkin, A. L. (1951) *Biol. Rev.* **26,** 339–409.
29. Slayman, C. L. (1977) in *Water Relations in Membrane Transport in Plants and Animals*, eds. Jungreis, A. M., Hodges, T. K., Kleinzeller, A. & Schultz, S. G. (Academic, London), pp. 69–86.